**Ministry Of Higher Education and Scientific Research**

**University of Babylon**

**College of Science**

**Department of Physics**

# Study of the Electronic and Optical Properties of Nickel-Oxide Nanoparticles

Submitted To the Council of The Department of Physics, College of Science, University of Babylon

In Partial Fulfilment of The Requirements for Bachelor Degree of Science in Physics

**By**

**Jaafar Ghanim Kareem**

**Supervised by**

**Assist. Prof. Dr. Mohammad G. Merdan**

بسم الله الرحمن الرحيم

**(وَإِذَا قِيلَ انشُزُوا فَانشُزُوا يَرْفَعِ اللَّهُ الَّذِينَ آمَنُوا مِنكُمْ وَالَّذِينَ أُوتُوا الْعِلْمَ دَرَجَاتٍ ۚ وَاللَّهُ بِمَا تَعْمَلُونَ خَبِيرٌ)**

صدق الله العلي العظيم

(سورة المجادلة : اية 11)

# Acknowledgments

I extend my sincere thanks to my professors in the Department of Physics, grateful for their help, advice, and moral support throughout the university career that I spent, asking God Almighty to preserve and guide them and make them an asset for future generations of students. Assist. Prof. Dr. Mohammad G. Merdan is the owner of high morals, kind words, wonderful advice, and abundance of knowledge. I thank him for helping us in completing our graduate research.

# Supervisor Certification

I certify that the dissertation entitled " Study of the Electronic and Optical Properties of Nickel-Oxide Nanoparticles" was prepared under my supervision at the Department of physics / College of Science /University of Babylon, as partial fulfillment of the requirements for bachelor's degree.

Signature:

Assist. Prof. Dr. Mohammad G. Merdan

Date:    /    / 2024

# Abstract

Nickel oxide (NiO) nanoparticles have garnered significant attention due to their unique optical and electrical properties, making them promising candidates for various applications such as solar cells, gas sensors, and catalysis. This study delves into the theoretical investigation of NiO nanoparticles using Density Functional Theory (DFT) to elucidate their electronic structure, optical response, and electrical conductivity. Additionally, the research explores various synthesis methods for NiO nanoparticles, analyzing their impact on the resulting properties.

DFT calculations will be employed to investigate the band structure, density of states, and optical absorption spectra of NiO nanoparticles. The influence of particle size, morphology, and defects on these properties will be examined. Furthermore, the electrical conductivity of NiO nanoparticles will be explored, considering factors such as doping and temperature dependence.

The study will encompass a comprehensive review of established and emerging synthesis methods for NiO nanoparticles, including sol-gel, hydrothermal, and chemical vapor deposition techniques. The advantages and limitations of each method will be discussed, with a focus on their ability to control particle size, morphology, and defect concentration. By correlating the theoretical findings with experimental results from the literature, this research aims to provide a deeper understanding of the structure-property relationships in NiO nanoparticles, paving the way for their optimized design and implementation in various technological applications.

# Table of Contents

# Chapter One

# General Introduction

## 1.1 Introduction

Nanotechnology refers to the branch of science and engineering dedicated to materials, having dimensions in the order of 100th of nm or less.

Nanocrystalline materials have attracted much attention because of their different magnetic, electric, dielectric, thermal, optical and catalytic properties in comparison to their bulk counterparts. Nanostructured metal oxides have been extensively studied due to both scientific interests and potential applications. Metal oxide nanoparticles (NPs) can adopt a large variety of structural geometries.

Furthermore, they incur electronic structures that may exhibit metallic, semiconducting or insulating characteristics, endowing them with diverse chemical and physical properties. Therefore, metal oxides are among the most important functional materials used for chemical and biological sensing and transduction[1].

NiO is an important transition metal oxide which has been of interest due to its interesting magnetic properties Bulk crystals of NiO possess a rhombohedral structure and exhibit antiferromagnetic behavior below 523 K Whereas it has a cubic (NaCl-type) structure and is paramagnetic above that temperature, it has been earlier suggested that fine particles of NiO should exhibit weak ferromagnetism or superparamagnetism[2].

NiO nanoparticles have been found to be promising as an electrode material for lithium-ion batteries. Nanosized NiO has demonstrated excellence properties such as catalytic, magnetic, electrochromic, optical and electrochemical properties. Furthermore, nickel oxides can be used as a transparent p-type semiconducting layer and are being studied for applications in smart windows, electrochemical supercapacitors and dye-sensitized photocathodes. For technological applications, a detailed understanding of the size, morphology and interparticle interactions of nanoscale NiO could be important.

A great many methods have been employed to synthesize NiO nanoparticles such as evaporation, electrodeposition, thermal decomposition and sol–gel techniques [3].
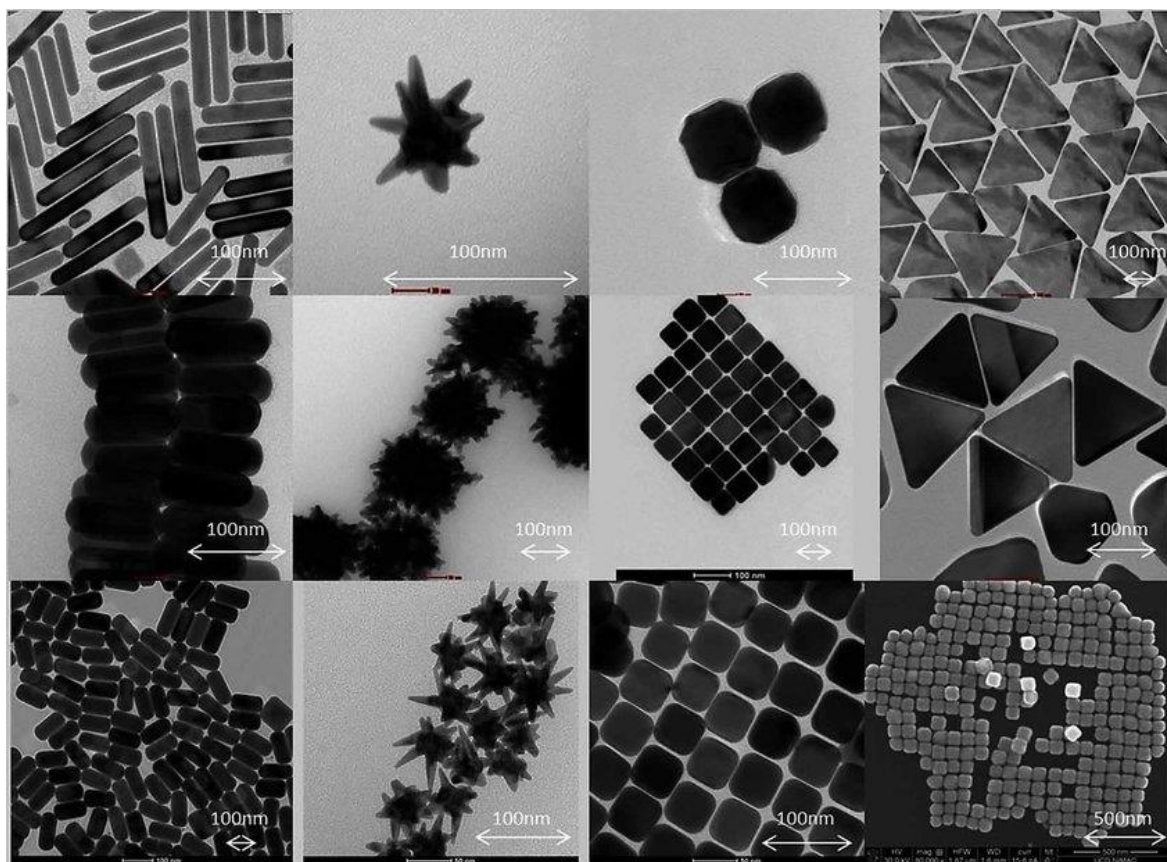
**Figure (1-1):** TEM and SEM micrographs nanoparticles

## 1.2 Properties of Nickel-Oxide Nanoparticle

Nickel oxide is a semiconductor material available in the form of a green crystalline powder. It has a wide and direct energy gap and, in addition to its optical, electrical and magnetic properties, is also very important because of its excellent chemical stability. It has been used as an antiferromagnetic material. This feature exhibits the properties of symmetrical crystals with high chemical stability and thermodynamics. It has good oxidation resistance. It is one of the materials that change color when an electric field is applied to it. It has a density (6.67 g/cm) and a molecular weight (842.87 g/mol), its melting point is (1984°C) and it has a positive electrical conductivity (p-type). The manufacturing effort is low and it is also a material that enables the storage of ions. It is characterized by good durability and the possibility of manufacturing using a number of techniques. It is a

material that is transparent to ultraviolet, visible and near-infrared rays and is often used as transparent electrodes and windows. Photovoltaics as well as fuel cells, displays and other electronic devices [4].

## 1.2.1 Structural Properties

Nickel oxide is a chemical compound with the formula NiO and known as nickel (II) oxide. It has a cubic (FCC) crystalline structure, and it is similar to the crystalline structure of sodium chloride (NaCl), as (Ni) has a valence of (+2) and Oxygen (-2) , and Figure (1.1) shows the crystal structure of nickel oxide, where Oxygen ions ($O^{-2}$) is at the vertices of the cube in addition to the centers of the faces, and nickel ions ($Ni^{+2}$) are in the center and middle of the sides of the cube, where ($O^{-2}$) forms a face-centered cubic cell "FCC" and ($Ni^{+2}$) ions represent the closest neighbors. The ionic radii of nickel and oxygen are estimated to be $R(O^{-2})$ = 140 pm and $R(Ni^{+2})$ = 72 pm. [4].
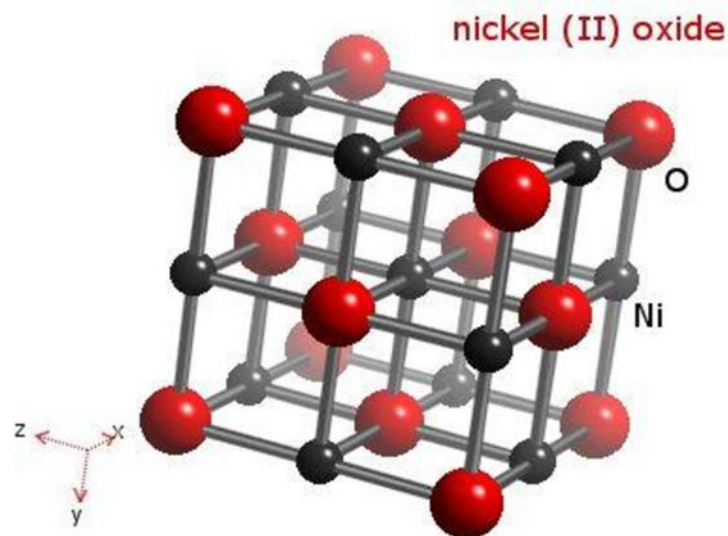
**Figure (1-2):** Nickel-Oxide crustal structure

The oxygen atom occupies the position (1/2,1/2,1/2) with respect to the nickel reference atom Ni (0,0,0). And the (100) plane is a common plane consisting of 50% nickel and 50% oxygen, while the (111) plane is alternating, and the (111) face is polar. Therefore, it is

unstable, unlike the (100) face. It is nonpolar, so it is stable. Table (1.1) shows the lattice properties of nickel oxide [4].

**Table (1-1):** Lattice parameters of Nickel-Oxide

| Lattice | Parameters |
|---------|------------|
| a (Å) | 4.17 |
| b (Å) | 4.17 |
| c (Å) | 4.17 |
| α | 90 |
| β | 90 |
| γ | 90 |

## 1.2.2 Optical Properties

The compound of Ni-O is a transparent semiconductor to ultraviolet (UV), visible, and near-infrared rays. The transparency of nickel oxide in the visible range is related to its valence, and asymmetric nickel oxide appears less permeable than stoichiometric nickel oxide, and this is due to the presence of $Ni^{+3}$. As for the value the index of refraction is about 1.6-2.33.

 for the figure indicate that the transmittance of ultraviolet and visible light through a thin layer of nickel oxide is very related to the temperature and the degree of oxidation. It explains that the transmittance at (350°C) is not clear, so for layers of (NiO) through 2.5h and a temperature of (450°C) the transmittance takes a Maximum value of (80% - 70%)in the range of wavelengths (1000 nm-500 nm) [4].
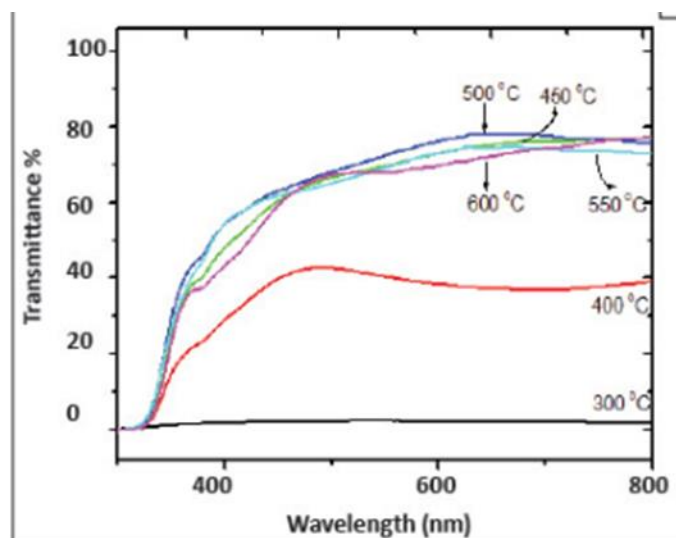
**Figure (1-3):** Transmittance spectra obtained for NiO films for 2.5h
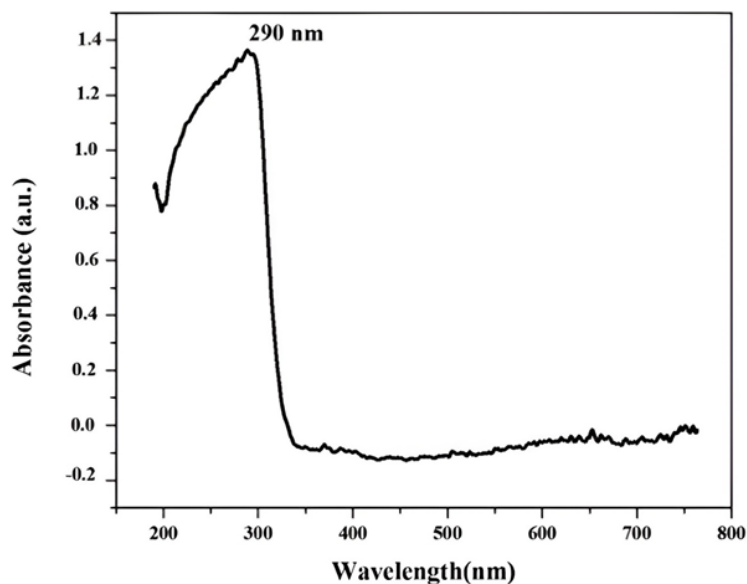


**Figure (1-4):** UV-Visible absorption spectrum of NiO nanoparticles

**Figure (1-4)** shows the absorption spectra of NiO nanoparticles using a UV-Vis spectrophotometer at temperatures ranging from 200 to 800 nm. According to this, the cut-off wavelength for the current spectrum's absorption spectrum is 290 nm, with the highest absorption occurring at that wavelength.

The absorption gradually increases across the visible spectrum while it continues to diminish until the end of the UV zone. As a result, these nanoparticles would have higher transmittance and could be useful in opto-electric applications [5].

The coefficient, k and refractive index, n of sol-gel NiO films have been determined from the spectrophotometric data using the following relations:

$$\alpha = \frac{1}{d} \ln \left( \frac{1}{T} \right) \tag{1.1}$$

$$k = \frac{\alpha \lambda}{4\pi} \tag{1.2}$$

$$n = \left( \frac{1-R}{1+R} \right) + \sqrt{\frac{4R}{(1-R)^2} - k^2} \tag{1.3}$$

where R is the film reflectance (substrate reflectance is subtracted), λ is the wavelength of the incident beam, and α is the absorption coefficient. The low values of extinction reveal the good transparency of the studied films. The extinction coefficient of 200 °C treated film is below 0.03 (400–700 nm). The extinction coefficient is higher for NiO films treated at 300–500 °C, but their values are below 0.21 in the visible spectral range [6].



(a)                                              (b)
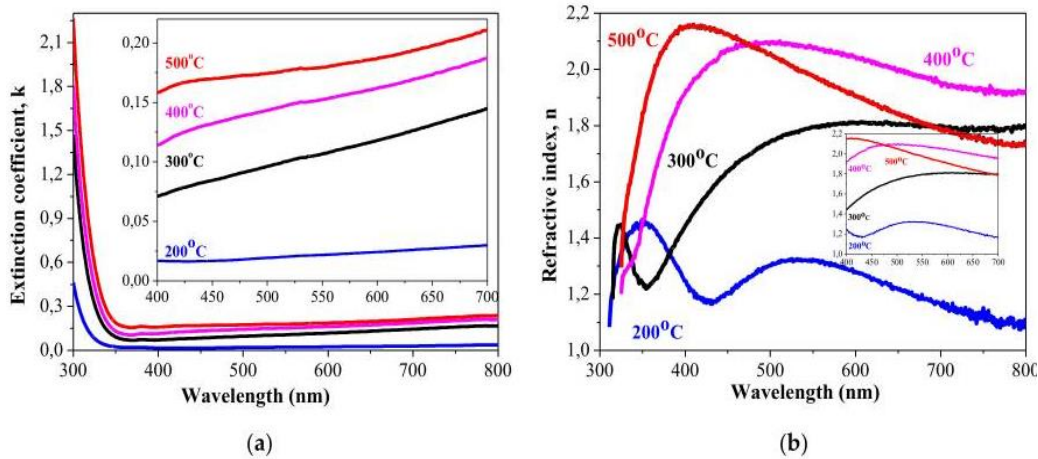
**Figure (1-5):** Extinction coefficient (a) and refractive index (b) of sol-gel NiO films. It can be seen that 200 °C film possess a refractive index of 1.24 at 630 nm and increases to 1.81 (300 °C), 2.02 (400 °C), and 1.86 (500 °C)[6].

7

**Table (1-2):** The optical band gap and refractive index values of NiO films, deposited by various methods.

| Optical Band Gap (eV) | Refractive Index | Spectral Range | Deposition Method |
|---|---|---|---|
| 3.572 | 2.15 | Average 280-900nm | Spray pyrolysis |
| 3.63 | - | - | Thermal evaporation |
| 3.40 | - | (Aqueous solution) | Chemical spray |
| 4.00 | - | (Alcoholic solution) | Chemical spray |
| 3.25-4.00 | 1.871 | 550nm | Spray pyrolysis |
| 3.78-3.85 | >2 | 450-800 nm | Sol-gel |
| 3.73 | 1.82-1.42 | 300-800 nm | Sol-gel |
| 3.47-3.86 | - | - | Sol-gel |
| 3.12-3.93 | 2.0-1.4 | 300-1000 nm | Magnetron sputtering |
| 3.945 | 2.2-1.9 | 400-1000 nm | e-beam technique |
| 3.14-3.83 | 2.8-1.8 | 300-1000 nm | Spray pyrolysis |
| 3.50-3.81 | 2.10-1.45 | 300-1000 nm | Wet method |

## 1.2.3 Electronic Properties

Nickel oxide is non-insulating at room temperature and is an antiferromagnetic material. It also has a wide energy gap. and is one of the most important electronic materials after tungsten oxide. It is used in making electrical anodes and has several uses Due to its high electronic efficiency, nickel oxide also has high stability, is highly durable, can be coated,

and has a positive (p-type) conductivity [4]. In order to evaluate electrical properties of pure NiO. The resistance (R) is obtaining from the I-V measurements. The DC electrical conductivity values were measured for using the following formula:

$$\sigma_{dc} = \frac{1}{R} \times \frac{I}{A}$$

where R is the measured resistance, A is the cross-section area and I is the pellet thickness.

$\sigma_{dc}$ of NiO by I-V measurements is $3.70 \times 10^{-5}$ S.cm$^{-1}$[5].

**Table (1-3):** Sheet resistance values of sol-gel NiO films treated at temperatures from 200 to 500 °C.

| Annealing Temperature [°C] | Sheet Resistance [Ω/sq] |
|:---:|:---:|
| 200 | - |
| 300 | 689 |
| 400 | 690 |
| 500 | 689 |

The sheet resistivity of NiO films was measured by a four-point probe system, and the results are summarized along with annealing temperature in **Table (1-3).**

Results show that the samples after thermal treatment at 200 °C exhibit very low intrinsic conductivity. Increasing the temperature at and above 300 °C, NiO manifests p-type conductivity.

The WF of NiO thin films could be altered by different deposition techniques and the depositional parameters along with defects, such as oxygen vacancies or surface impurities, and composition.

**Table (1-4):** Work Functions of sol-gel NiO films, treated at different annealing temperatures.

| Annealing Temperature [°C] | Work function [eV] |
|---|---|
| 200 | 4.44 |
| 300 | 5.92 |
| 400 | 5.25 |
| 500 | 5.24 |

**Table (1-4)** shows that the work function changes slightly with increasing annealing temperature (with the exception of the sample annealed at 200 °C)[6].

## 1.3 Preparation Methods of Nickel-Oxide Nanoparticles

### 1.3.1 Chemical Precipitation

The main materials were nickel nitrate hex hydrate (Ni (NO3)2·6H$_2$O), sodium hydroxide (NaOH), polyvinylpyrrolidone (PVP, MW = 65000), polyethylene glycol (PEG, MW = 15000), and cetyl trimethyl ammonium bromide (CTAB).

First, we prepared two separate solutions; one a solution of 8.7 g of nickel nitrate in 60 mL of deionized water and the other contains a solution of 3.0 g sodium hydroxide in 150 mL of deionized water. Amount of 1 g of mentioned surfactants in three different experiments added to latter solution. Next, the former solution was added dropwise into the later. The mixed solution was stirred by magnetic stirring apparatus (1000 rpm) at room temperature. The resultant light-green solution was filtered, and then washed with deionized water and ethanol for 5–10 times and was dried at 50∘C for 24 hours, then calcined at 300∘C, 450∘C, and 600∘C for 2 hours for three different samples. The surfactants were removed after the

mentioned processes. Main reactions occur during the experimental procedure can be written briefly as follows:

$$2NaOH_{(s)} \longrightarrow 2Na^+_{(aq)} + 2OH^-_{(aq)}$$

$$Ni(NO_3)_2 \cdot 6H_2O_{(s)} \longrightarrow Ni^{2+}_{(aq)} + 2NO_3^-_{(aq)} + 6H_2O_{(aq)},$$

$$Ni^{2+}_{(aq)} + 2OH^-_{(aq)} + xH_2O_{(aq)} \longrightarrow Ni(OH)_2 \cdot xH_2O_{(s)} \downarrow,$$

$$Ni(OH)_2 \cdot xH_2O_{(s)} \xrightarrow{50-100} Ni(OH)_{2(s)} + xH_2O_{(g)} \uparrow,$$

$$Ni(OH)_{2(s)} \xrightarrow{300} NiO_{(s)} + H_2O_{(g)} \uparrow.$$
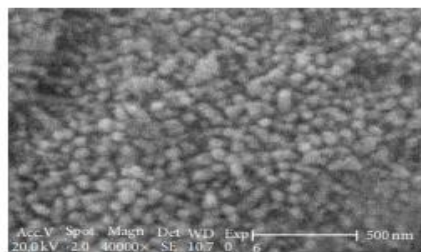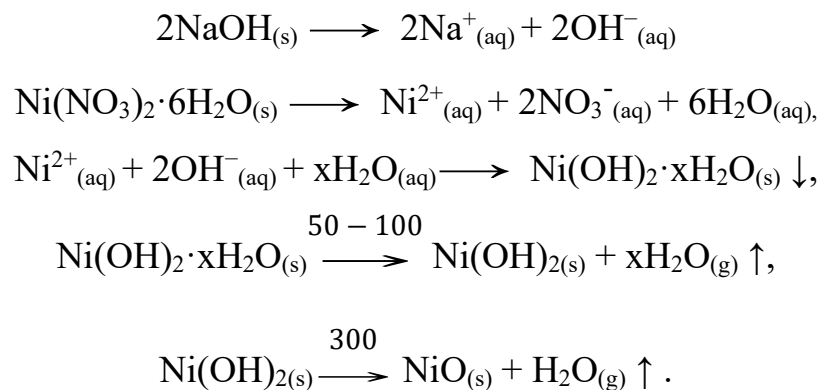
(a)
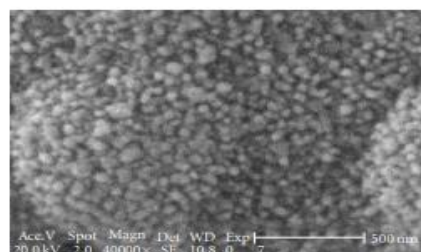
(b)
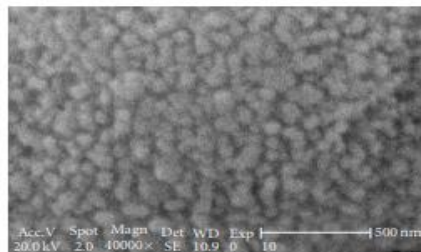
(c)

**Figure (1-6):** The SEM image of NiO nanoparticles. (a) PVP, (b) PEG, and (c) CTAB [7].

## 1.3.2 Hydrothermal Synthesis

NiO nanostructures were formed by the hydrothermal synthesis route of nickel acetate, $Ni(CH_3COO)_2$.

All the chemicals and solvents used during the synthesis are analytic grade reagents and were used as received without any further purification. Distilled water (DW) was used throughout the experiment. For the synthesis of NiO NPs, the first 0.5 g of nickel acetate was dissolved in 100 mL of DW. Next, the solution was mixed under constant magnetic stirring to ensure homogeneity. Then, the solution was transferred into a 50 mL capacity Teflon-lined stainless-steel auto-clave, sealed and put in an oven whose temperature is maintained at 180 °C for 24 h. Finally, the autoclave was cooled to room temperature and the resulting greenish precipitate formed was washed with DW first (to remove any excess ions), and then with ethanol, dried in an oven at 60 °C for 5 h to obtain the NiO NPs [8].
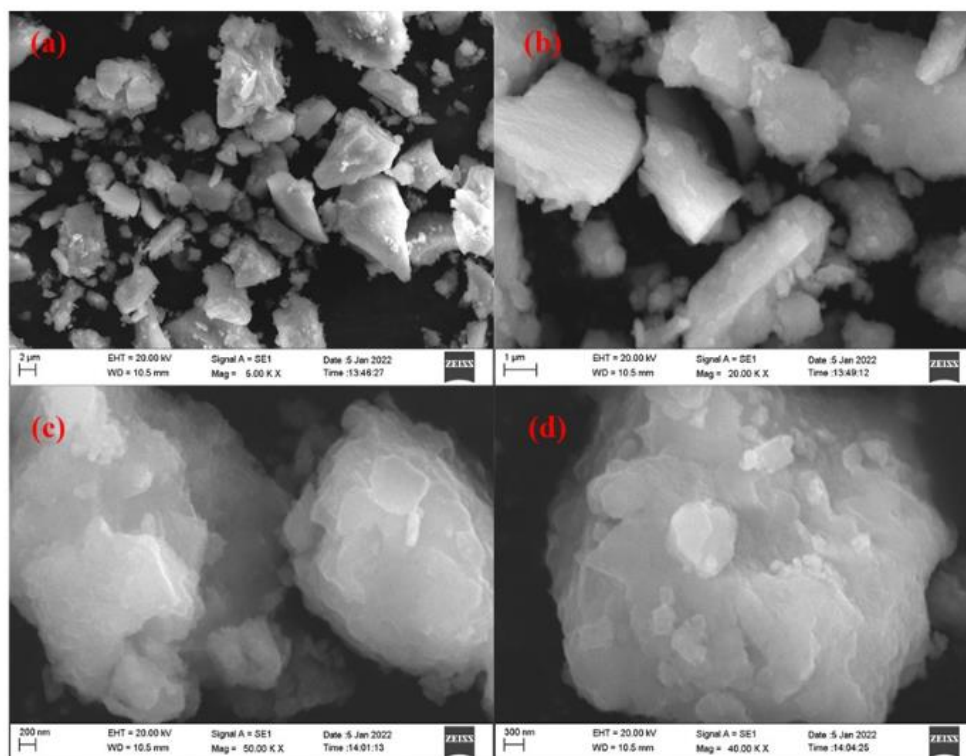


**Figure (1-7):** SEM images at different magnifications (a-d) of NiO NP.

### 1.3.3 Sol-Gel Method

NiO nanoparticles were prepared by a surfactant-mediated method using nonionic copolymer F108 as an organic template material. Poly(alkylene oxide) block copolymer F108 with 1 g was dissolved in 10 ml of anhydrous ethanol.

Different amounts of water ($H_2O$) (0, 10, 20, 40 mass%) were added to dilute the ethanol solution. 0.01 mole of nickel nitrate ($Ni(NO_3)_2 \cdot 6H_2O$) was then added to the F108 ethanol solution and stirred vigorously for 1 h. The role of the block copolymer in the as-made sample was used to control the growth of nanoparticles and coat the nanoparticles to prevent them from further oxidation and aggregation. These nanoparticles were easily dispersed in ethanol to form a homogeneous colloidal solution. The resulting sol solutions were aged and dried at 343 K in an oven for 48 h. The asmade sample was then calcined at various temperatures (623,723, 823, 923 K) for 3 h to remove the copolymer. The nanostructure of NiO nanoparticles was then investigated by thermogravimetric analysis (SETSYS Evolution TGA, Thermal Analysis System). Powder XRD data was measured with a Rigaku D/max-IV diffractometer with CuKα radiation ($\lambda = 0.15418$ nm). The sample was scanned from 20 to 80° (2 θ) in steps of 4°/min. A SEM image was obtained using a Hitachi 3000N, and the sample was prepared by dispersing the final powder in conductive glue, and this dispersion was then sprayed with carbon. The TEM micrographs were made with a FEI E.O Tecnai F20 G2 MAT S-TWIN transmission electron microscope operated at 200 keV. The sample for TEM was prepared by dispersing the final powder in ethanol, and this dispersion was then dropped on carbon-copper grids. The N2 adsorption-desorption isotherm was recorded on a Micromeritics ASAP 2010 automated sorption analyzer. The sample was outgassed for 7 h at 423 K before the analysis. The Barrett-Joyner-Halenda (BJH) model and the BrunauerEmmett-Teller (BET) methods were applied to determine the pore size and BET surface area, respectively. FTIR spectra, in the

range of 4000-400 $cm^{-1}$ were recorded on a PerkinElmer Spectrum GX infrared spectrophotometer [9].

## 1.4 Applications of Nickel-Oxide Nanoparticles

- In preparation of nickel cermet for the anode layer of solid oxide fuel cells.
- In lithium nickel oxide cathodes for lithium-ion micro batteries.
- In electrochromic coatings, plastics and textiles.
- In nanowires, nanofibers and specific alloy and catalyst applications.
- As a catalyst and as anti-ferromagnetic layers.
- In light weight structural components in aerospace.
- Adhesive and coloring agents for enamels.
- In active optical filters.
- In ceramic structures.
- In automotive rear-view mirrors with adjustable reflectance.
- In cathode materials for alkaline batteries.
- Electro chromic materials.
- Energy efficient smart windows.
- P-type transparent conductive films.
- Materials for gas or temperature sensors, such as CO sensor, H2 sensor, and formaldehyde sensors.
- As a counter electrode.
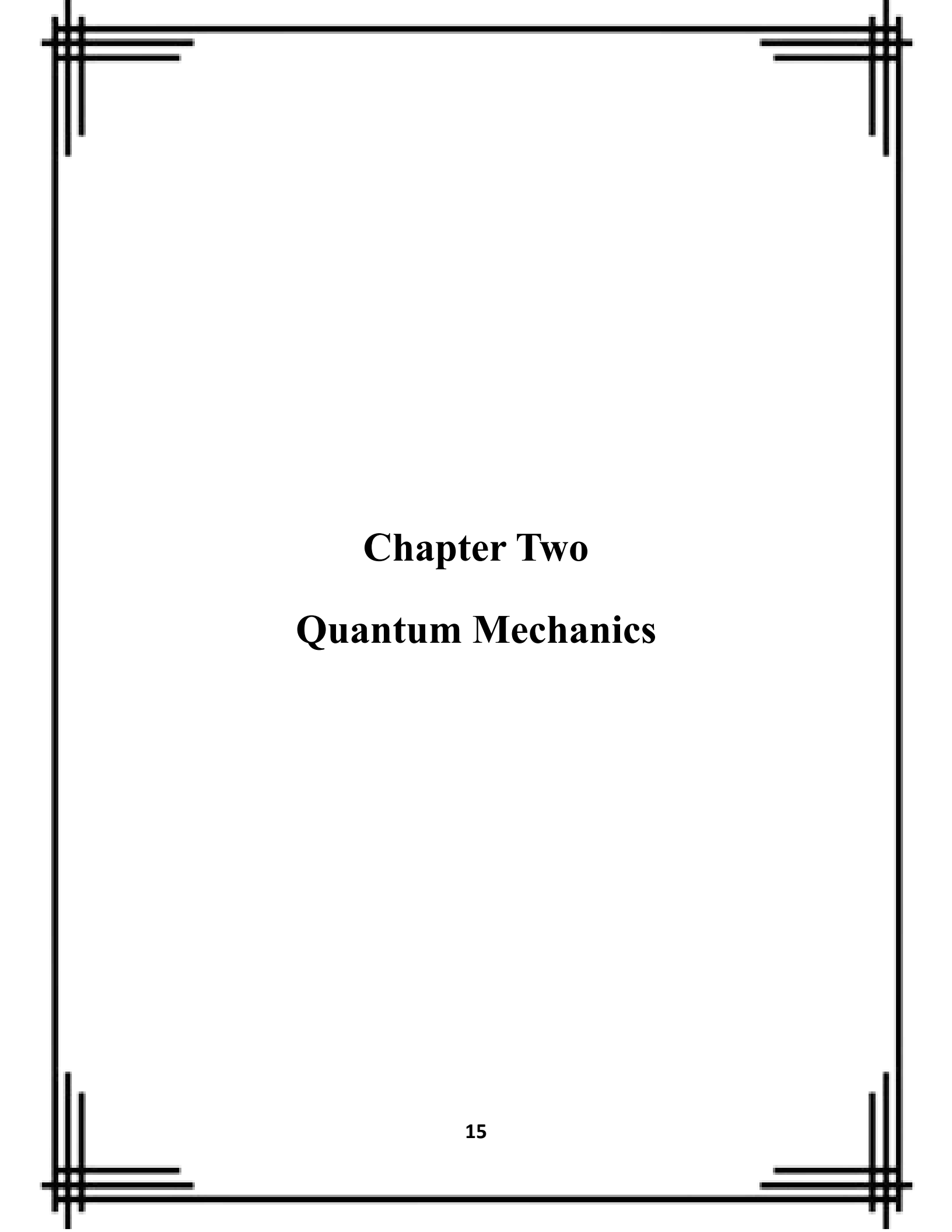
# Chapter Two

# Quantum Mechanics

## 2.1 A Brief History

**1900 (Planck):** Max Planck proposed that light with frequency $v$ is emitted in quantized lumps of energy that come in integral multiples of the quantity,

$$E = hv = \hbar\omega \tag{2.1}$$

where h $\approx 6.63 \cdot 10^{-34}$ J ·s is Planck's constant, and $\hbar = h/2\pi = 1.06 \cdot 10^{-34}$ J·s.

The frequency $v$ of light is generally very large (on the order of $10^{15}$ s$^{-1}$ for the visible spectrum), but the smallness of $h$ wins out, so the $hv$ unit of energy is very small (at least on an everyday energy scale). The energy is therefore essentially continuous for most purposes.

However, a puzzle in late 19th-century physics was the blackbody radiation problem. In a nutshell, the issue was that the classical (continuous) theory of light predicted that certain objects would radiate an infinite amount of energy, which of course can't be correct. Planck's hypothesis of quantized radiation not only got rid of the problem of the infinity, but also correctly predicted the shape of the power curve as a function of temperature. Planck's hypothesis simply adds the information of how many lumps of energy a wave contains. Although strictly speaking, Planck initially thought that the quantization was only a function of the emission process and not inherent to the light itself.

**1905 (Einstein):** Albert Einstein stated that the quantization was in fact inherent to the light, and that the lumps can be interpreted as particles, which we now call "photons." This proposal was a result of his work on the photoelectric effect, which deals with the absorption of light and the emission of elections from a material.

$E = pc$ for a light wave. (This relation also follows from Einstein's 1905 work on relativity, where he showed that $E = pc$ for any massless particle, an example of which is a photon.) And we also know that $\omega = ck$ for a light wave. So, Planck's relation $E = hv = \hbar\omega$ becomes

$$E = \hbar\omega \Rightarrow pc = \hbar(ck) \Rightarrow p = \hbar k \qquad (2.2)$$

This result relates the momentum of a photon to the wavenumber of the wave it is associated with.

**1913 (Bohr):** Niels Bohr stated that electrons in atoms have wavelike properties. This correctly explained a few things about hydrogen, in particular the quantized energy levels that were known.

**1924 (de Broglie):** Louis de Broglie proposed that all particles are associated with waves, where the frequency and wavenumber of the wave are given by the same relations we found above for photons, namely $E = \hbar\omega \Rightarrow p = \hbar(k)$. The larger $E$ and $p$ are, the larger $\omega$ and $k$ are. Even for small $E$ and $p$ that are typical of a photon, $\omega$ and $k$ are very large because $\hbar$ is so small. So, any everyday-sized particle with large (in comparison) energy and momentum values will have extremely large $\omega$ and k values. This (among other reasons) makes it virtually impossible to observe the wave nature of macroscopic amounts of matter.

The fact that any particle has a wave associated with it leads to the so-called wave-particle duality. Are things particles, or waves, or both? Well, it depends what you're doing with them. Sometimes things behave like waves, sometimes they behave like particles. A vaguely true statement is that things behave like waves until a measurement takes place, at which point they behave like particles.

**1925 (Heisenberg):** Werner Heisenberg formulated a version of quantum mechanics that made use of matrix mechanics. We won't deal with this matrix formulation (it's rather difficult), but instead with the following wave formulation due to Schrodinger.

**1926 (Schrodinger):** Erwin Schrodinger formulated a version of quantum mechanics that was based on waves. He wrote down a wave equation (the so-called Schrodinger equation) that governs how the waves evolve in space and time. Even though the equation is correct,

the correct interpretation of what the wave actually meant was still missing. Initially Schrodinger thought (incorrectly) that the wave represented the charge density.

**1926 (Born):** Max Born correctly interpreted Schrodinger's wave as a probability amplitude. By "amplitude" we mean that the wave must be squared to obtain the desired probability. More precisely, since the wave (as we'll see) is in general complex, we need to square its absolute value. This yields the probability of finding a particle at a given location (assuming that the wave is written as a function of x). This probability isn't a consequence of ignorance, as is the case with virtually every other example of probability you're familiar with. For example, in a coin toss, if you know everything about the initial motion of the coin (velocity, angular velocity), along with all external influences (air currents, nature of the floor it lands on, etc.), then you can predict which side will land facing up. Quantum mechanical probabilities aren't like this.

They aren't a consequence of missing information. The probabilities are truly random, and there is no further information (so-called "hidden variables") that will make things un-random. The topic of hidden variables includes various theorems (such as Bell's theorem) [10].


## 2.2   Double Slit Experiment

If monochromatic light or wavelength is directed towards a barrier with two slits, the distance between them which is equal to the wavelength of the light used, the original wave is divided into two new waves, each of which enters through one of the two slits and is emitted from it. Thus, interference occurs for the waves emanating from the two slits, and a pattern appears on the screen called the interference pattern. The bright areas of the pattern represent the meeting of two peaks, and the dark areas of the pattern represent the
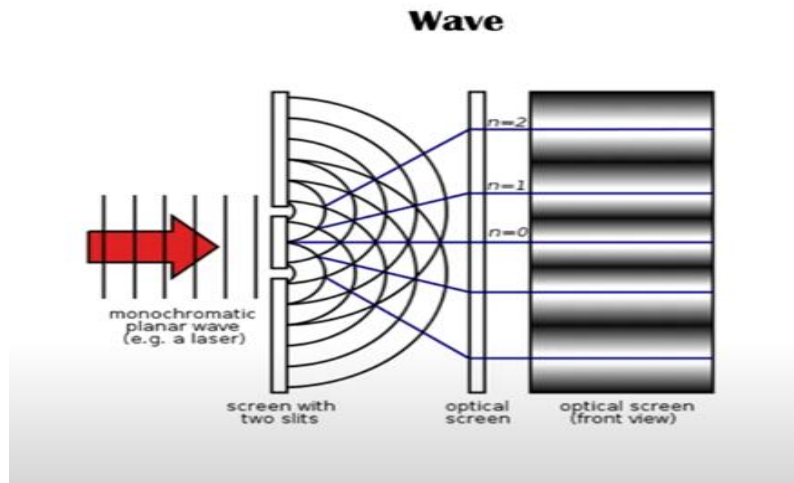
**Figure (2-1):** Wave nature of light

meeting of two troughs as in **Figure (2-1).** We know that this phenomenon is due to the wave nature of light.
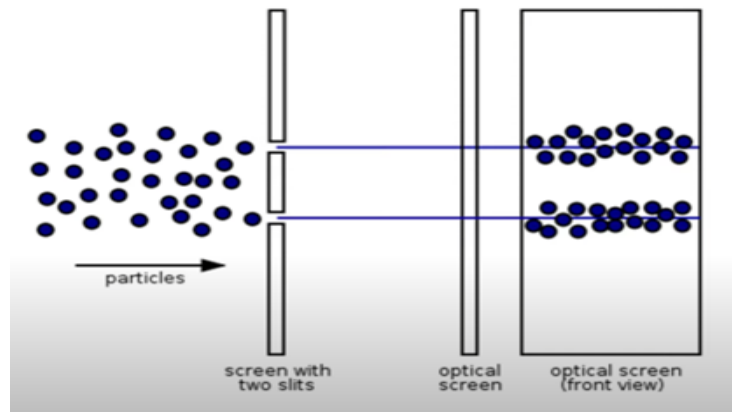


**Figure (2-2):** What was expected for the particles to behave

Scientists replaced the light wave with particles (electrons, for example). It was assumed that these particles would pass through the cracks and take a shape identical to the shape of the cracks (two vertical lines) on the barrier, as in **Figure (2-2).**
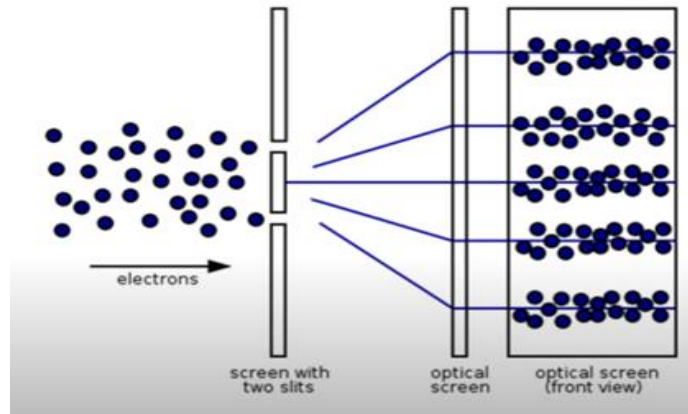
**Figure (2-3):** Wave nature for the particles

But instead, an interference pattern appeared on the screen identical to the wave interference pattern, even though there were no waves to interfere with. This strange phenomenon led scientists to assume that the interference occurred as a result of particles colliding with each other, forming an interference pattern as in waves as we see in **Figure (2-3).**

Then, a low-intensity source was used to release one particle each time towards the two slits. It is logical that this particle will pass through one of the cracks and settle on the screen in a specific position. It was initially observed that these particles settle in random places on the screen, and the explanation for this matter is that these particles suffer from deviations and breakages on their way to the screen, so they take random places.
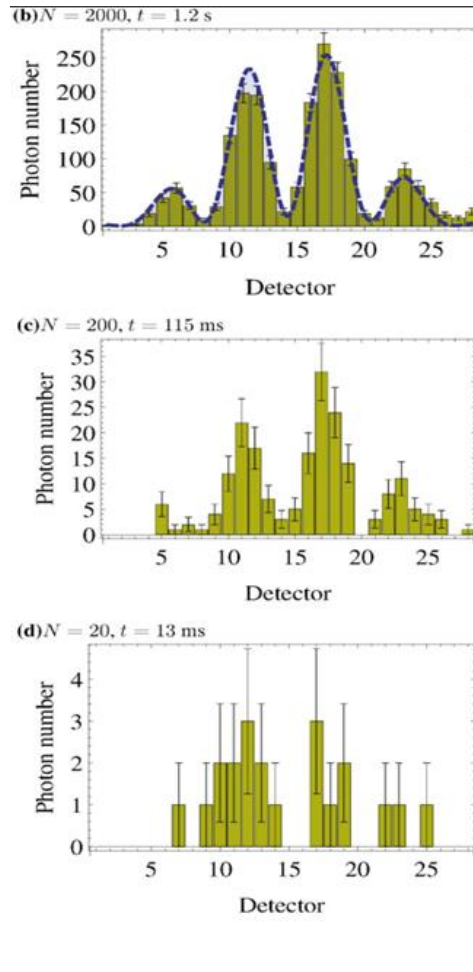
**Figure (2-4):** Particles distribution over time

But with the passage of time and the large number of individual particles passing through, it became apparent that the locations of these particles are not random, but rather each of them has a specific location as shown in **Figure (2-4),** so that the interference pattern appears again without there being anything to interfere with.

A theory was proposed to solve this dilemma by the two scientists, Niels Bohr and Heisenberg, and this theory was called the Copenhagen interpretation. The significance of this interpretation was that no particle (photon, electron, atoms...) can be described as a single particle and it moves in a physical manner, but rather it is in the form of a wave pattern. The probability function is called the wave function.

Since the particle is present in all places of its wave function at the same time, when the particle is launched towards the two slits, its travel path is in the form of a wave function, as it passes through one of the two slits and at the same time passes through the other slit in the same proportion under the influence of quantum correlation and entanglement, where the probabilities of the particle's existence interfere with each other[11].

## 2.3   The Schrödinger Wave Equation

The Schrödinger equation has two 'forms', one in which time explicitly appears, and so describes how the wave function of a particle will evolve in time. In general, the wave function behaves like a wave, and so the equation is often referred to as the time dependent Schrödinger wave equation. The other is the equation in which the time dependence has been 'removed' and hence is known as the time independent Schrödinger equation and is found to describe, amongst other things, what the allowed energies are of the particle. These are not two separate, independent equations – the time independent equation can be derived readily from the time dependent equation[10].

### 2.3.1   The Time Dependent Schrödinger Wave Equation

The classical nonrelativistic expression for the energy of a particle, which is the sum of the kinetic and potential energies. We'll assume as usual that the potential is a function of only $x$. We have

$$E = K + V = \frac{1}{2} mv^2 + V(x) = \frac{p^2}{2m} + V(x). \tag{2.3}$$

We'll now invoke de Broglie's claim that all particles can be represented as waves with frequency $\omega$ and wavenumber $k$, and that $E = \hbar\omega$ and $p = \hbar k$. This turns the expression for the energy into

22

$$\hbar\omega = \frac{\hbar^2 k^2}{2m} + V(x). \tag{2.4}$$

A wave with frequency $\omega$ and wavenumber $k$ can be written as usual as $\psi(x,t) = Ae^{i(kx-\omega t)}$. In 3-D we would have $\psi(r, t) = Ae^{i(k \cdot r - \omega t)}$ We now note that

$$\frac{\partial \psi}{\partial t} = -i\omega\psi \implies \omega\psi = i\frac{\partial \psi}{\partial t}, \quad \text{and}$$

$$\frac{\partial^2 \psi}{\partial x^2} = -k^2\psi \implies k^2\psi = -\frac{\partial^2 \psi}{\partial x^2}. \tag{2.5}$$

If we multiply the energy equation in Eq. (2.4) by $\psi$, and then plug in these relations, we obtain

$$\hbar(\omega\psi) = \frac{\hbar^2}{2m}(k^2\psi) + V(x)\psi \implies \boxed{i\hbar\frac{\partial \psi}{\partial t} = \frac{-\hbar^2}{2m} \cdot \frac{\partial^2 \psi}{\partial x^2} + V\psi} \tag{2.6}$$

This is the time-dependent Schrodinger equation. If we put the $x$ and $t$ arguments back in, the equation takes the form, [10].

$$i\hbar\frac{\partial \psi(x,t)}{\partial t} = \frac{-\hbar^2}{2m} \cdot \frac{\partial^2 \psi(x,t)}{\partial x^2} + V(x)\psi(x,t). \tag{2.7}$$

### 2.3.2 The Time Independent Schrödinger Wave Equation

The time dependence entered into the wave function via a complex exponential factor exp[$-iEt/\hbar$]. This suggests that to 'extract' this time dependence we guess a solution to the Schrödinger wave equation of the form

$$\Psi(x,t) = \psi(x)e^{-iEt/\hbar} \tag{2.8}$$

Where the space and the time dependence of the complete wave function are contained in separate factors.

If we substitute this trial solution into the Schrödinger wave equation, and make use of the meaning of partial derivatives, we get

$$-\frac{\hbar^2}{2m}\frac{d^2\psi(x)}{dx^2}e^{-iEt/\hbar}+V(x)\psi(x)e^{-iEt/\hbar}=i\hbar.-iE/\hbar e^{-iEt/\hbar}\psi(x)=E\psi(x)e^{-iEt/\hbar}. \quad (2.9)$$

We now see that the factor exp[−iEt/ℏ] cancels from both sides of the equation, giving us

$$-\frac{\hbar^2}{2m}\frac{d^2\psi(x)}{dx^2}+V(x)\psi(x)=E\psi(x) \quad (2.10)$$

If we rearrange the terms, we end up with

$$\frac{\hbar^2}{2m}\frac{d^2\psi(x)}{dx^2}+\left(E-V(x)\right)\psi(x)=0 \quad (2.11)$$

which is the time independent Schrödinger equation[12].

## 2.4 Density Functional Theory (DFT)

Density functional theory (DFT) is a quantum-mechanical (QM) method used in chemistry and physics to calculate the electronic structure of atoms, molecules and solids. It has been very popular in computational solid-state physics since the 1970s. However, it was not until the 1990s that improvements to the method made it acceptably accurate for quantum-chemical applications, resulting in a surge of applications. The real forte of DFT is its favourable price/performance ratio compared with electron-correlated wave function-based methods such as Møller–Plesset perturbation theory or coupled cluster. Thus, larger

(and often more relevant) molecular systems can be studied with sufficient accuracy, thereby expanding the predictive power inherent in electronic structure theory. As a result, DFT is now by far the most widely used electronic structure method[13].

Advantage of DFT originates with the fact that the electron density has three spatial coordinates, regardless of the number of electrons in the chemical system. Thus, DFT allows the calculation of structures and properties of molecules with a couple of hundred atoms, a feat not generally possible with high-level WFT methods[14].

The many-body character of the electron-electron interactions requires further simplification and the next transformation constitutes the fundament of DFT: the Schrödinger Equation is expressed for an equivalent system of independent electrons characterized by single-electron wave functions $\varphi_i(r)$ and whose electron density is the same as the one of the systems with interacting electrons. Two theorems by Hohenberg and Kohn show that the single-particle charge density $n(r)$ can be chosen as the fundamental variable for the description of the ground state of a system of interacting electrons. This density $n(r)$ is only a function of the three space coordinates, which simplifies greatly the many-body problem. The two theorems by Hohenberg and Kohn are as follows:

1. All physical quantities are a functional of the electron density $n(r)$ of the system, in particular the total energy.
2. The physical (or « real ») electron density of a system is the one minimizing the total energy functional of the system (variational principle).

$$E[n] = -\frac{1}{2}\sum_i \int \varphi_i^*(\mathbf{r})\nabla^2\varphi_i(\mathbf{r})d\mathbf{r} + \frac{1}{2}\iint \frac{n(\mathbf{r})n(\mathbf{r}')}{|\mathbf{r}-\mathbf{r}'|}d\mathbf{r}d\mathbf{r}' + \int V_{ext}(\mathbf{r},\mathbf{R})\,n(\mathbf{r})\,d\mathbf{r} + E_{xc}[n(\mathbf{r})] \quad (2.12)$$

where the first term corresponds to the kinetic energy of non-interacting electrons.

The corrections to this term due to the many-body interaction of the electrons are included in the last term, the exchange-correlation term. The second term corresponds to the electron

Coulomb interactions. The Coulomb interactions between electrons and nuclei are included in the external potential term $V_{est}$(r,R)[15].

The electron charge density is determined from the single electron wave functions $\varphi_i$(r) according to the expression:

$$n(\mathbf{r}) = \sum_i^N \left|\varphi_i(\mathbf{r})\right|^2 \tag{2.13}$$

with N the number of occupied states for all atoms of the system. The minimization of the energy functional relative to the electron density yields an eigenvalue problem, called the Kohn-Sham Equation (2.13), which has the form of a single-particle Schrödinger Equation:

$$\left(-\frac{\hbar^2}{2m}\nabla^2 + V_{\text{eff}}(\mathbf{r})\right)\varphi_i(\mathbf{r}) = \varepsilon_i\,\varphi_i(\mathbf{r}) \tag{2.14}$$

The effective potential $V_{\text{eff}}$ is given by:

$$V_{\text{eff}}(\mathbf{r}) = V_{\text{ext}}(\mathbf{r},\mathbf{R}) + \int \frac{n(\mathbf{r}')}{|\mathbf{r} - \mathbf{r}'|}\,d\mathbf{r}' + v_{xc}(\mathbf{r}) \tag{2.15}$$

with $v_{xc}$ the exchange-correlation potential defined by:

$$v_{xc}(\mathbf{r}) = \frac{\partial E_{xc}}{\partial n(\mathbf{r})} \tag{2.16}$$

## 2.5 Local Density Approximation (LDA)

The local density approximation (LDA) (Parr and Yang, 1989) represents the simplest approach to $E_{XC}[\rho 0]$, which, in the context of this model, would be given by

$$E_{XC}^{LDA}[\rho_0] = \int \rho_0(r)\varepsilon_{XC}(r)dr \tag{2.17}$$

where $\varepsilon_{XC}$(r) is the exchange-correlation energy per electron of a homogenous electron gas (a system formed by uniformly distributed electrons moving on a positive charge background so that the system is electrically neutral) whose electronic density is precisely ρ0(r) at each point r. The term "local" refers to the absence of any ρ0(r) derivative in the expression for $E_{XC}[\rho 0]$ given by Eq. (2.17), which implies that the LDA approximation will

be valid when the electronic density varies very slowly with the position (see next paragraph). If the exchange and correlation contributions are considered separately, the first one can be computed analytically. The correlation energy, in turn, lacks an analytical expression and is represented as a complicated function of $\rho 0$ depending of parameters whose values are fitted using accurate simulations for the energy of the homogeneous electron gas as reference[16].

## 2.6 Generalized Gradient Approximation (GGA)

In the generalized gradient approximation (GGA) to DFT, the XC potential depends on the electron density $\rho$ and its gradient $\nabla\rho$ and is a complicated function in three-dimensional space. This makes an analytical solution of the XC integrals impossible and numerical quadrature is used to compute the XC matrix elements,

$$V_{\mu\nu}^{XC(GGA)} = \int d\mathbf{r}\, \varphi_\mu(\mathbf{r}) v_{XC}^{GGA}(\mathbf{r}) \varphi_\nu(\mathbf{r}) \approx \sum_k w_k \varphi_\mu(\mathbf{r}_k) v_{XC}^{GGA}(\mathbf{r}_k) \varphi_\nu(\mathbf{r}_k), \qquad (2.18)$$

where $r_k$ are the quadrature points and $w_k$ the corresponding weights. The numerical XC quadrature is perfectly suited for parallelization and Yasuda was the first to exploit GPUs for this purpose. He adopted a strategy in which the computationally less demanding steps in the quadrature (grid generation, evaluation of $v_{XC}^{GGA}$ on the grid points) are done in DP on the CPU while the expensive steps are done on the GPU. These are the evaluation of $\rho$ and $\nabla\rho$ on the grid points and the summation of Eq. (2.18) which can be formulated as matrix-vector multiplications and dot products[17].
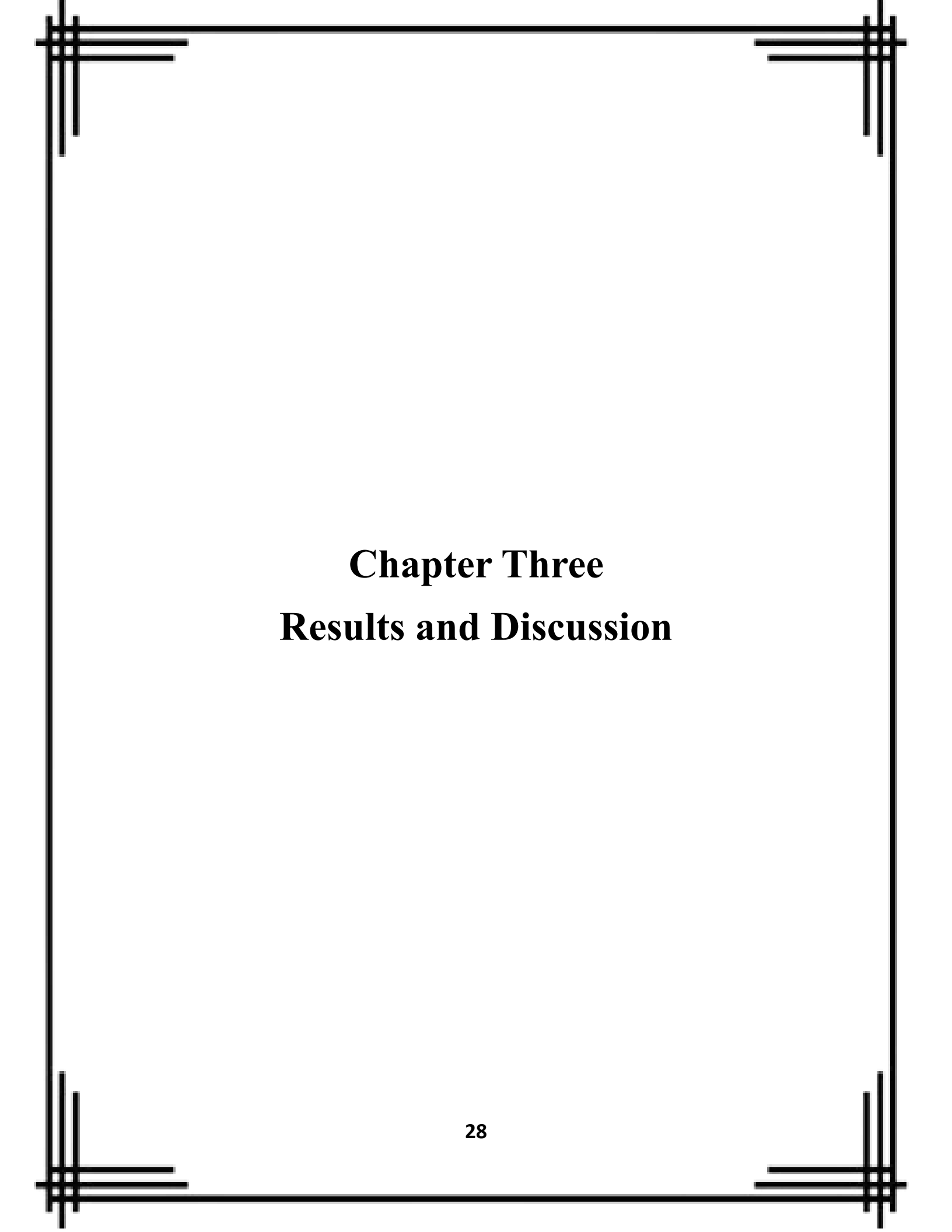
# Chapter Three
# Results and Discussion

## 3.1  Introduction

Nickel oxide (NiO) is a fascinating material with diverse applications in various fields, including electronics, catalysis, energy storage, and sensors. This research delves into the fascinating world of NiO nanoparticles, exploring their band gap, structural properties, and optical properties.

The band gap of a material is the energy difference between its valence and conduction bands. It plays a crucial role in determining its electrical conductivity, optical properties, and potential applications. The band gap of NiO nanoparticles can vary depending on their size, shape, and synthesis method. NiO has a direct band gap of around 3.6-4.0 eV. The band gap of NiO nanoparticles can be tuned by controlling their size, shape, and doping. This tunability makes them attractive for various applications, such as solar cells, LEDs, and gas sensors.

NiO nanoparticles can exist in various crystal structures, including cubic, hexagonal, and mixed phases. The most common structure is the rock salt (NaCl) structure, which is cubic. In this structure, each Ni ion is surrounded by six O ions, and vice versa. The size and shape of NiO nanoparticles can be controlled by adjusting the synthesis parameters. Transmission electron microscopy (TEM) is commonly used to characterize the size and shape of NiO nanoparticles. X-ray diffraction (XRD) is used to determine the crystal structure and phase purity of the nanoparticles.

The optical properties of NiO nanoparticles are closely related to their band gap and structural properties. NiO nanoparticles exhibit strong absorption in the ultraviolet (UV) region and visible light region. The absorption peak is typically located around 350-400 nm, which corresponds to the band gap energy. NiO nanoparticles also exhibit photoluminescence (PL) properties. When excited with UV light, they emit light in the

visible region. The PL emission peak is typically located around 500-600 nm. The PL properties of NiO nanoparticles can be influenced by their size, shape, and surface defects.

## 3.2   Method and Calculations

The first-principles density functional theory (DFT) within Plane-Wave Pseudopotential within the Generalized Gradient Approximation (GGA) implemented in the ABINIT code was used to calculate electronic and optical properties of B-HgS. The Brillouin zone was performed automatically with 6x6x6 k-point mesh according to Monkhorst-pack scheme.

## 3.3   Results and Discussion

### 3.3.1   Density of State

The DOS is a property that is used extensively in quantum systems in condensed matter physics; it refers to the energy level of the electrons, photons, or phonons in a solid crystal. The electronic DOS quantifies how "packed" the electrons in a quantum mechanical system are in energy levels. The DOS can vary from zero for an energy level that is inaccessible to the electrons, with no space occupied by them, to a defined occupation value at a specific energy level that is accessible to the electrons of the material. There is a direct correlation between the concept of quantized energy levels that is described by quantum mechanics and the DOS. The DOS is an energetic configuration due to the wave property of matter. In some systems, the interatomic spacing, the crystal structure, and the atomic charge of the material only allow electrons of certain wavelengths to propagate in the system, which also limits the possible directions of wave propagations. Each wave occupies a different mode or state that can have the same wavelength or the same quantized energy levels. This determines the degeneracy of states with the same energy and the

absence of states in other energies that are incompatible with the system in which no space is occupied by the system. In the case of electronic states, the DOS permits the calculation of the number of electrons for each energy level, and the diagram of these states defines the electrical conduction properties of a material. DOS is usually denoted with one of the symbols *g, ρ, n,* or *N*.
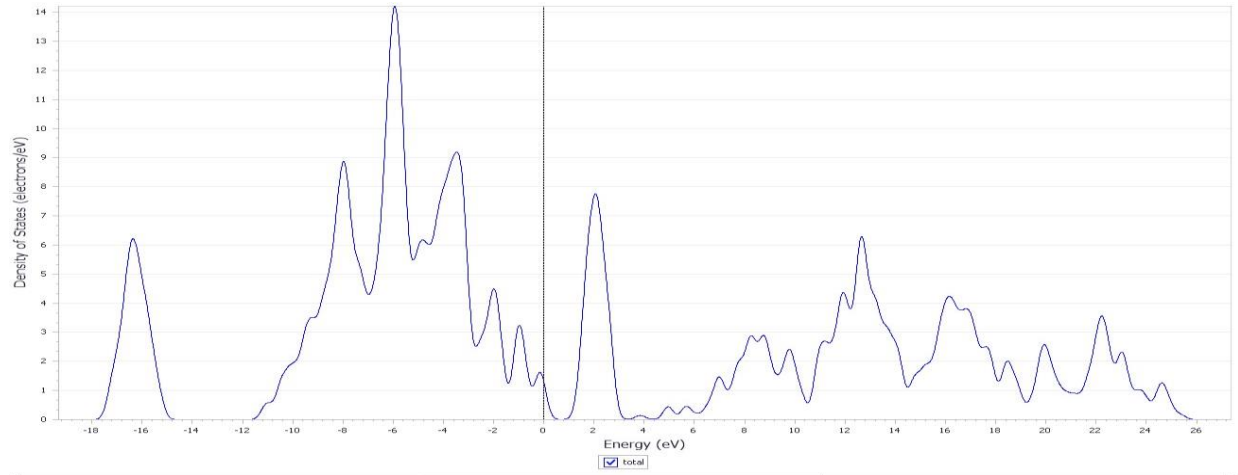


**Figure (3-1):** Density of state of NiO

### 3.3.2   Band Structure

The band structure of a solid is a cornerstone concept in condensed matter physics, providing a comprehensive framework for understanding the electronic properties of materials. It arises from the interaction of individual atomic orbitals within a solid, leading to the formation of allowed energy bands separated by forbidden gaps.

Metals possess overlapping valence and conduction bands, enabling electrons to move freely and exhibit high electrical conductivity. Semiconductors, characterized by small band gaps, require an external energy input to excite electrons from the valence band to the conduction band, allowing them to conduct electricity under specific conditions. Insulators,

with large band gaps, effectively confine electrons within the valence band, resulting in negligible electrical conductivity.

The band structure serves as a powerful tool for predicting and tailoring the electrical, optical, and magnetic properties of materials. By manipulating the band structure through doping or engineering nanostructures, scientists can design materials with specific functionalities for applications in electronics, energy storage, and sensing technologies.

the calculated band gap is 3.695eV which agrees with the experimental values that ranged between 3.12eV and 4eV as it depends on the preparation method as shown in **Table(1-2)**.
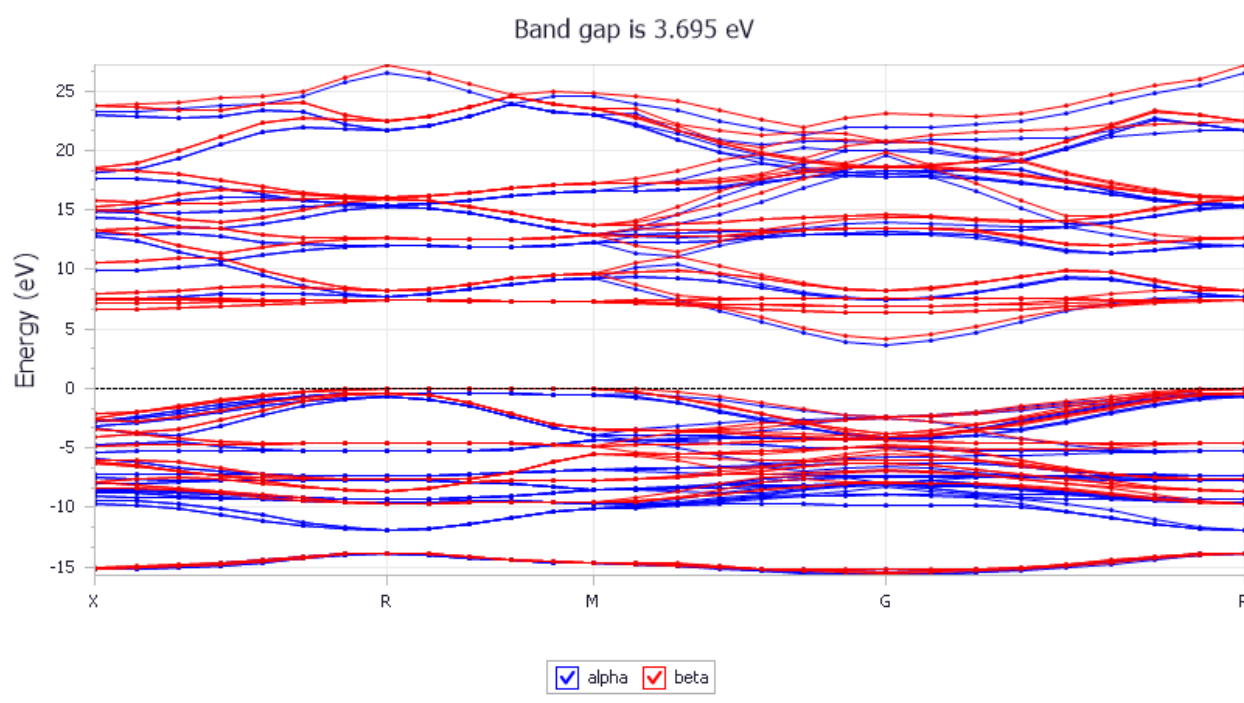
**Figure (3-2):** Band gap of NiO

### 3.3.3 Optical Properties

**1-Reflectivity:** Reflectivity is the ability of a material to reflect incident light, bouncing it back into the surrounding environment. It is a crucial optical property that determines how much light a material absorbs and how much it reflects. The reflectivity of a material depends on its surface characteristics, the angle of incidence of light, and the wavelength of light. Smooth, polished surfaces tend to reflect light more efficiently than rough, uneven surfaces. Additionally, materials with high refractive indices, such as metals, generally exhibit higher reflectivity than materials with low refractive indices, such as water.

We noticed that the reflectivity reaches a maximum value when the light wavelength is 700nm and higher.
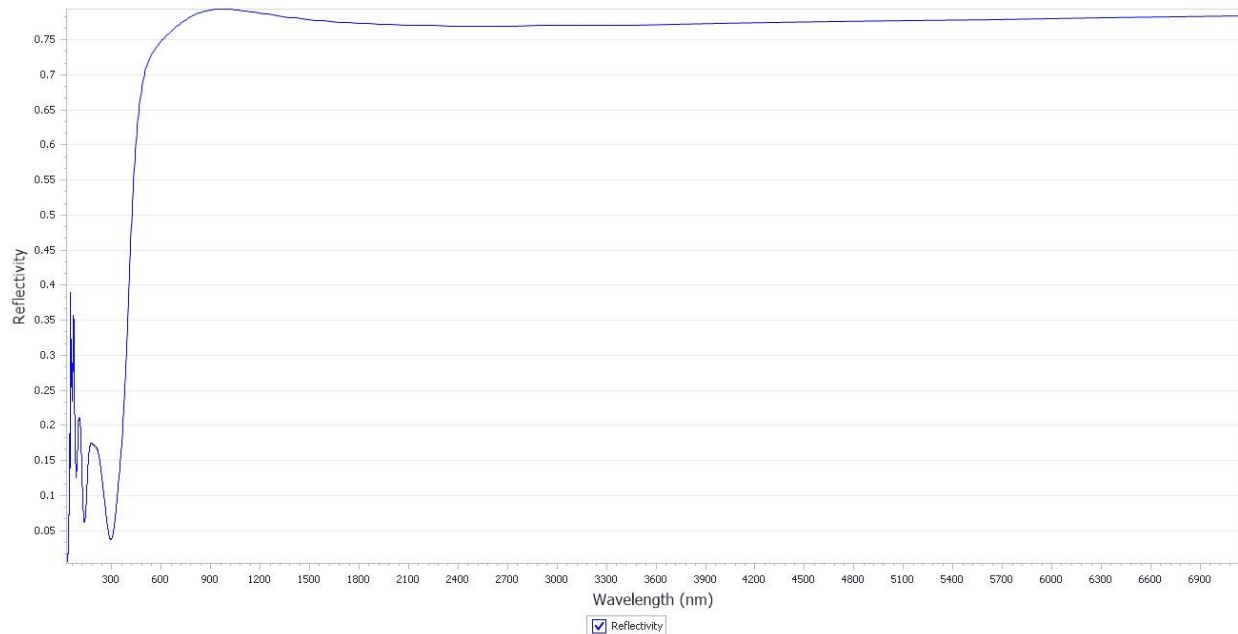


**Figure (3-3):** Reflectivity of NiO with respect to the wavelength
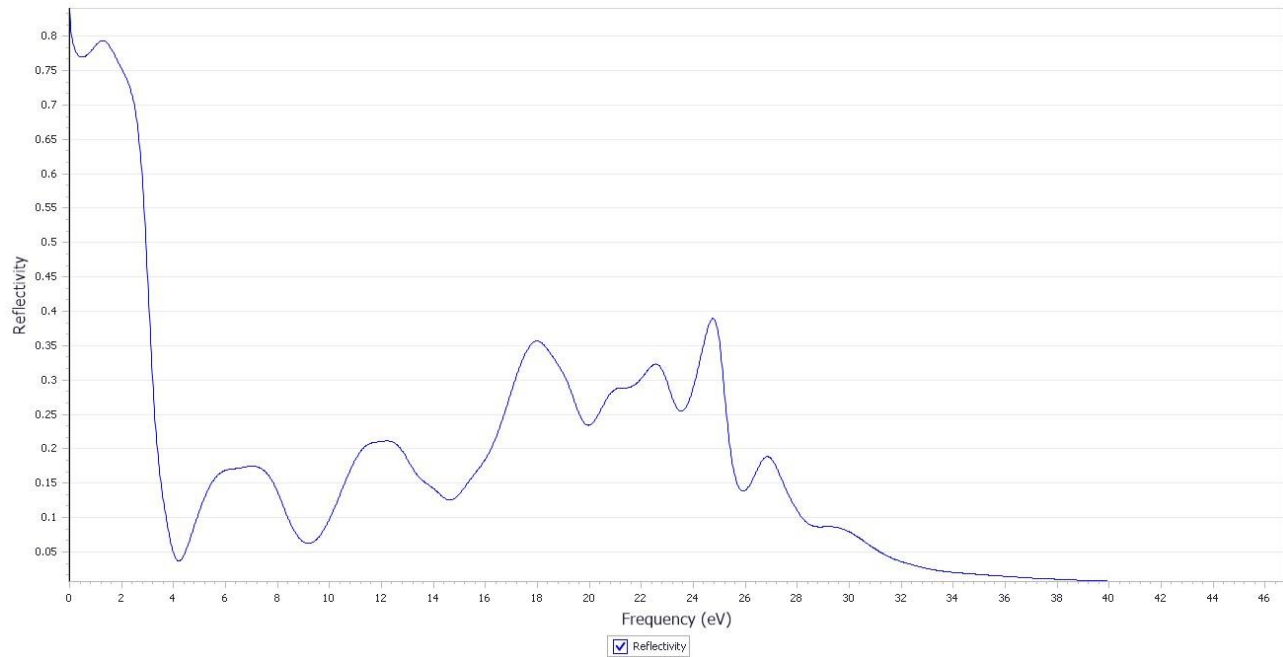
**Figure (3-4):** Reflectivity of NiO with respect to the frequency

**2- Absorption:** Absorption is a fundamental process where materials interact with light, capturing its energy and converting it into other forms. When light strikes a material, its constituent particles, such as electrons and atoms, absorb the energy of photons, causing them to jump to higher energy levels. The extent of absorption depends on the material's properties, the wavelength of light, and its intensity. Some materials, like black surfaces, readily absorb light across a broad spectrum, while others, like transparent materials, allow light to pass through with minimal absorption.

We can see from the figure below that the maximum absorption is at frequency of 18 eV and it's a good matching with the experimental values.
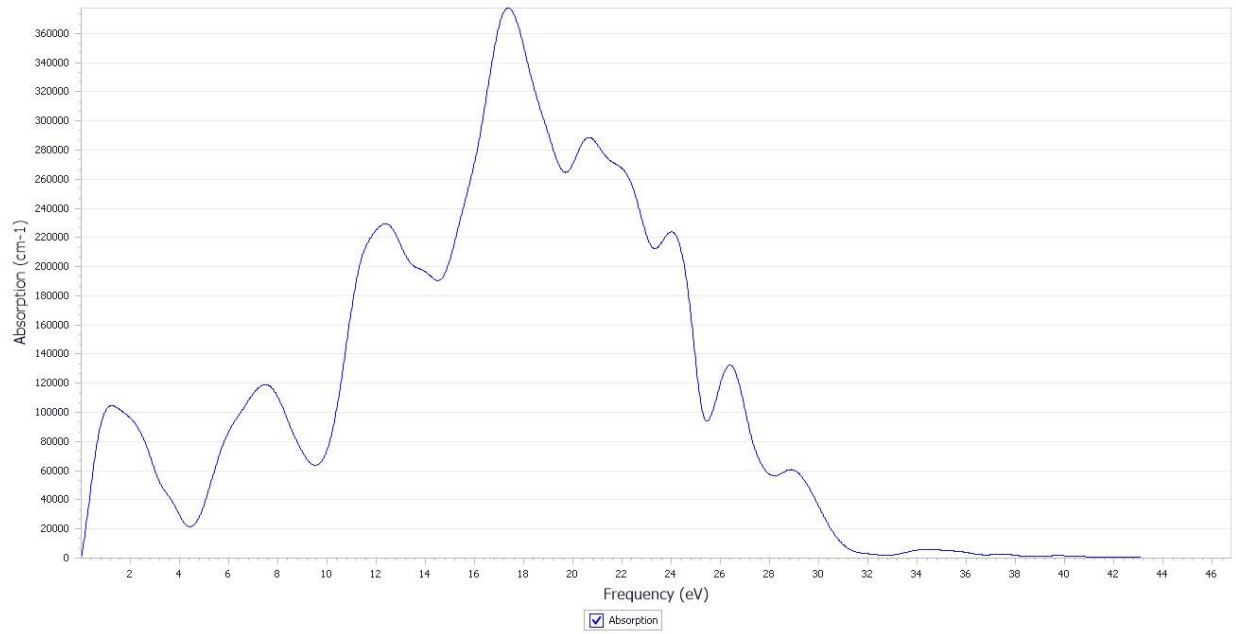
**Figure (3-5):** Absorption of NiO with respect to the frequency
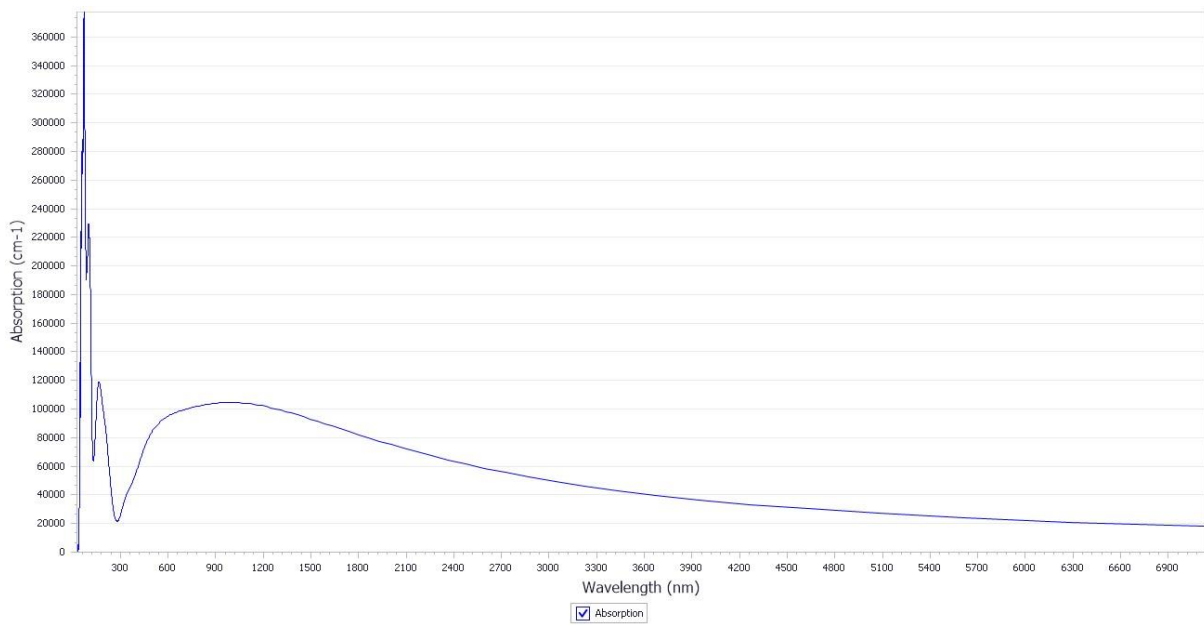


**Figure (3-6):** Absorption of NiO with respect to the wavelength

**3-Refractive Index:** The refractive index of a material quantifies how much light bends as it enters the material from another medium. It is a dimensionless quantity, typically denoted by the symbol 'n', representing the ratio of the speed of light in a vacuum to the speed of light in the material. The refractive index of a material is influenced by its density, molecular structure, and the wavelength of light. Denser materials and materials with higher polarizability tend to have higher refractive indices. Additionally, the refractive index of a material varies with the wavelength of light, a phenomenon known as dispersion.

As shown in the experimental values in **Table (1-2)**, the calculated refractive index ranged between 1.8 and 2.9 for the wavelengths from 300nm to 1200nm and it kept increasing as the wavelength increases and it depends on the preparation method.
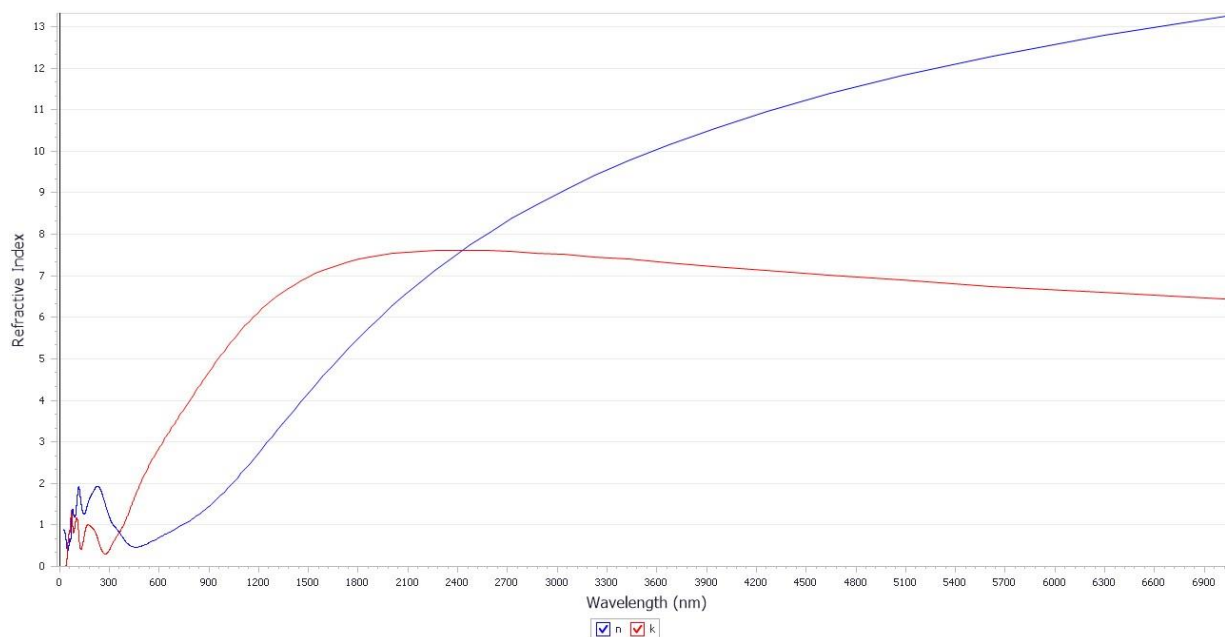


**Figure (3-7):** Refractive index of NiO with respect to the wavelength
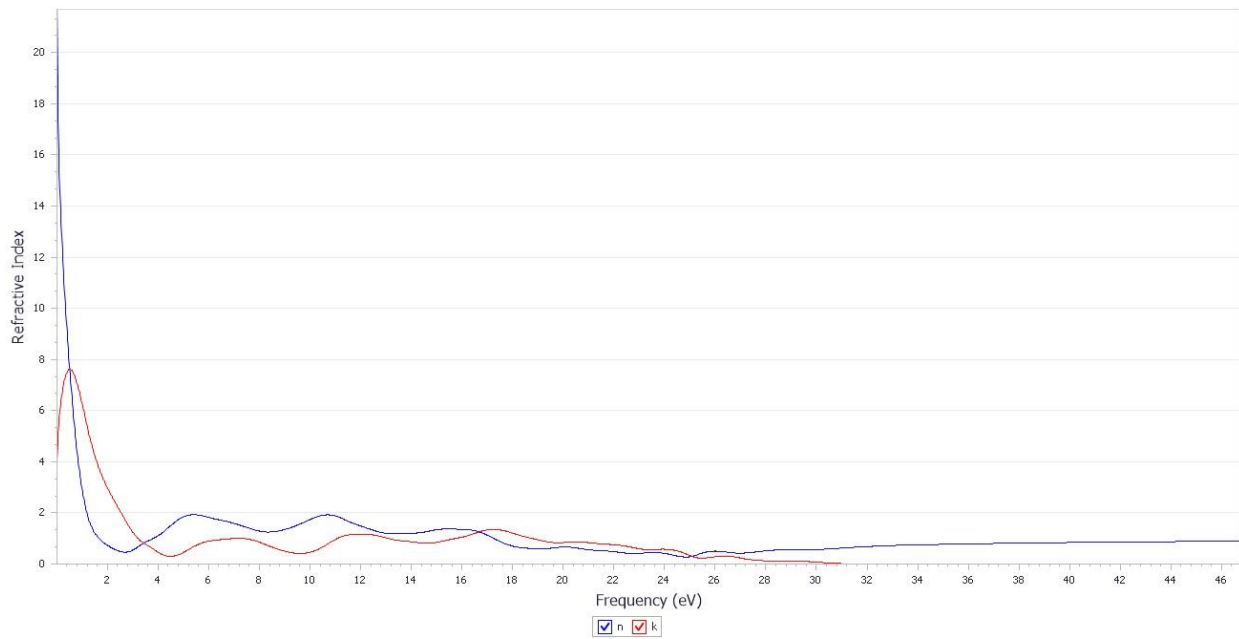
**Figure (3-8):** Refractive index of NiO with respect to the frequency

**4-Conductivity:** Optical conductivity is the property of a material which gives the relationship between the induced current density in the material and the magnitude of the inducing electric field for arbitrary frequencies.

This linear response function is a generalization of the electrical conductivity, which is usually considered in the static limit, i.e., for time- independent or slowly varying electric fields.

While the static electrical conductivity is vanishingly small in insulators (such as diamond or porcelain), the optical conductivity always remains finite in some frequency intervals (above the optical gap in the case of insulators). The total optical weight can be inferred from sum rules. The optical conductivity is closely related to the dielectric function, the generalization of the dielectric constant to arbitrary frequencies.
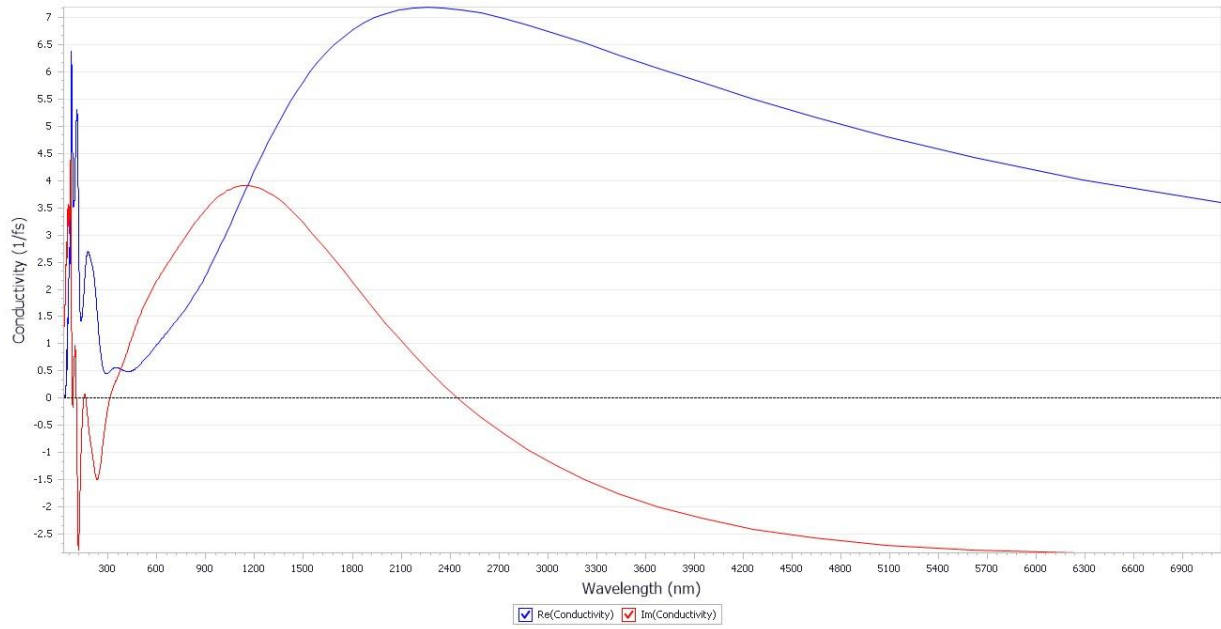
**Figure (3-9):** Conductivity of NiO with respect to the wavelength
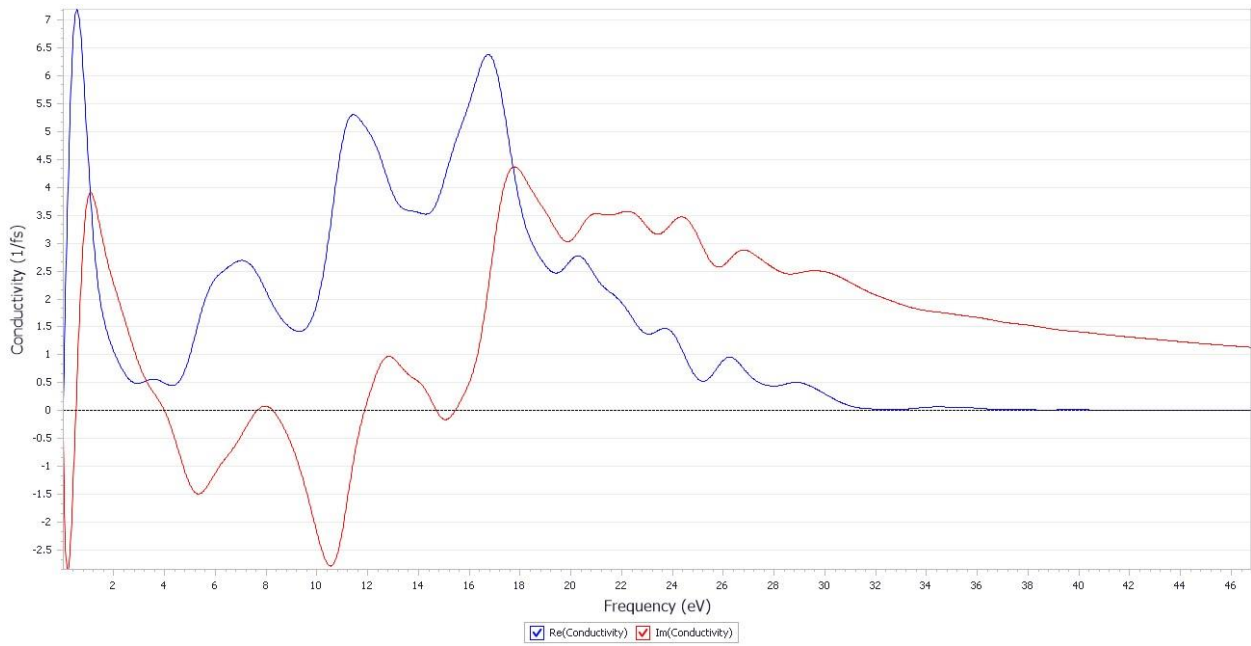


**Figure (3-10):** Conductivity of NiO with respect to the frequency

## 3.4 Conclusion

This study employed density functional theory (DFT) to investigate the optical and structural properties of nickel oxide (NiO).

The calculated results demonstrated a high degree of accuracy when compared to experimental data, validating the effectiveness of DFT in predicting the behavior of NiO. Specifically, the calculated lattice parameters and band gap energies exhibited strong agreement with experimental measurements.

This success underscores the ability of DFT to accurately capture the electronic and structural characteristics of NiO. The insights gained from this study contribute to a deeper understanding of NiO and its potential applications. The accurate prediction of its properties paves the way for further theoretical and experimental investigations, potentially leading to the development of novel materials and devices based on NiO.

Further research could explore the influence of external factors, such as doping or strain, on the properties of NiO using DFT. Additionally, investigating the surface properties of NiO with DFT could provide valuable information for applications in catalysis.

# References

[1]    M. Naseri *et al.*, "Structure and physical properties of NiO/Co3O4 nanoparticles," *Metals (Basel)*, vol. 6, no. 8, Aug. 2016, doi: 10.3390/met6080181.

[2]    T. Ahmad, K. V. Ramanujachary, S. E. Lofland, and A. K. Ganguli, "Magnetic and electrochemical properties of nickel oxide nanoparticles obtained by the reverse-micellar route," *Solid State Sci*, vol. 8, no. 5, pp. 425–430, May 2006, doi: 10.1016/J.SOLIDSTATESCIENCES.2005.12.005.

[3]    M. Salavati-Niasari, F. Davar, and Z. Fereshteh, "Synthesis of nickel and nickel oxide nanoparticles via heat-treatment of simple octanoate precursor," *J Alloys Compd*, vol. 494, no. 1, pp. 410–414, 2010, doi: https://doi.org/10.1016/j.jallcom.2010.01.063.

[4]    ف .ح. زينب and صص. صبرينة, "دراسة بعض الخصائص البصرية لأغشية أكسيد النيكل (NiO) المطعمة تطعيما مزدوجا بالنحاس (Cu)والكوبالت." 2023 ,17 .Nov :Accessed ,2020 ," [Online].                    Available:                    http://dspace.univ-eloued.dz:80/xmlui/handle/123456789/9779

[5]    M. Venkatachalapathy, N. Rajkamal, K. Sambathkumar, and G. Marudhu, "Synthesis, morphological, structural, functional, optical and computational properties of nickel oxide nanoparticles using hydrothermal method," *Dig J Nanomater Biostruct*, vol. 17, no. 4, pp. 1441–1451, doi: 10.15251/DJNB.2022.174.1441.

[6]    T. Ivanova, A. Harizanova, M. Shipochka, and P. Vitanov, "materials Nickel Oxide Films Deposited by Sol-Gel Method: Effect of Annealing Temperature on Structural, Optical, and Electrical Properties," 2022, doi: 10.3390/ma15051742.

[7]    M. Venkatachalapathy, N. Rajkamal, K. Sambathkumar, and G. Marudhu, "Synthesis, morphological, structural, functional, optical and computational properties of nickel

oxide nanoparticles using hydrothermal method," *Dig J Nanomater Biostruct*, vol. 17, no. 4, pp. 1441–1451, doi: 10.15251/DJNB.2022.174.1441.

[8]    Y. Bahari Molla Mahaleh, S. K. Sadrnezhaad, and D. Hosseini, "NiO nanoparticles synthesis by chemical precipitation and effect of applied surfactant on distribution of particle size," *J Nanomater*, vol. 2008, no. 1, 2008, doi: 10.1155/2008/470595.

[9]    S. S. G. K. W. I. F. J. Anita Lett, "Hydrothermal Synthesis and Photocatalytic Activity of NiO Nanoparticles under Visible Light Illumination | Anita Lett | Bulletin of Chemical Reaction Engineering & Catalysis." Accessed: Nov. 17, 2023. [Online]. Available: https://journal.bcrec.id/index.php/bcrec/article/view/13680/7111

[10]   David Morin, "Introduction to quantum mechanics".

[11]   "The Double-Slit Experiment Cracked Reality Wide Open | Latest Science News and Articles | Discovery." Accessed: Dec. 07, 2023. [Online]. Available: https://www.discovery.com/science/Double-Slit-Experiment

[12]   A. Paige. Flora, A. F. Rex, and S. T. Thornton, "Student solutions manual for Thornton & Rex's Modern physics, fourth edition," p. 58, 2013.

[13]   T. Van Mourik, M. Bühl, and M. P. Gaigeot, "Density functional theory across chemistry, physics and biology," *Philosophical Transactions of the Royal Society A: Mathematical, Physical and Engineering Sciences*, vol. 372, no. 2011, Mar. 2014, doi: 10.1098/RSTA.2012.0488.

[14]   K. B. Lipkowitz and D. B. Boyd, "Reviews in Computational Chemistry," *Reviews in Computational Chemistry*, vol. 7, pp. 1–414, Jan. 2007, doi: 10.1002/9780470125847.

[15] C. Adamo, H. Chermette, and D. Loffreda, "International Journal of Quantum Chemistry: Preface," *Int J Quantum Chem*, vol. 110, no. 12, p. 2101, Oct. 2010, doi: 10.1002/QUA.22799.

[16] P. G. Jambrina and J. Aldegunde, "Computational Tools for the Study of Biomolecules," *Computer Aided Chemical Engineering*, vol. 39, pp. 583–648, Jan. 2016, doi: 10.1016/B978-0-444-63683-6.00020-4.

[17] A. W. Götz, T. Wölfle, and R. C. Walker, "Quantum Chemistry on Graphics Processing Units," *Annu Rep Comput Chem*, vol. 6, no. C, pp. 21–35, Jan. 2010, doi: 10.1016/S1574-1400(10)06002-0.

وزارة التعليم العالي والبحث العلمي

جامعة بابل ا كلية العلوم

قسم الفيزياء

**دراسة الخواص الالكترونية والبصرية لجزيئات اوكسيد النيكل النانوية**

بحث تخرج للطالب

**جعفر غانم كريم**

مقدم الى مجلس كلية العلوم في جامعة بابل لنيل شهادة البكالوريوس في علوم الفيزياء

**بإشراف**

**أ. م. د. محمد غانم مردان**